A Wearable, Bending-Insensitive Respiration Sensor Using Highly Oriented Carbon Nanotube Film

Thanh Nguyen[1], Toan Dinh[1,2], Van Thanh Dau[1], Canh-Dung Tran[2], Hoang-Phuong Phan[1], Tuan-Khoa Nguyen[1], Khac-Hong Nguyen[3], Foisal Abu Riduan[1], Pablo Guzman[1], Nam-Trung Nguyen[1], and Dzung Viet Dao[1,4]

[1]School of Engineering and Built Environment, Griffith University, Nathan, QLD, Australia

[2]School of Mechanical and Electrical Engineering, University of Southern Queensland, Toowoomba, QLD, Australia

[3]Austal Vietnam, Vietnam

[4]Queensland Micro-Nanotechnology Centre, Griffith University, Nathan, QLD, Australia

Abstract:

Recently, wearable electronics for health monitoring have been demonstrated with considerable benefits for early-stage disease detection. This article reports a flexible, bending-insensitive, bio-compatible and lightweight respiration sensor. The sensor consists of highly oriented carbon nanotube (HO-CNT) films embedded between electro-spun polyacrylonitrile (PAN) layers. By aligning carbon nanotubes between the PAN layers, the sensor exhibits a high sensitivity towards airflow (340 mV/(m/s)) and excellent flexibility and robustness. In addition, the HO-CNT sensor is insensitive to mechanical bending, making it suitable for wearable applications. We successfully demonstrated the attachment of the sensor to the human philtrum for real-time monitoring of the respiration quality. These results indicate the potential of HO-CNT flow sensor for ubiquitous personal health care applications.

Keywords

Airflow sensor , carbon nanotube , respiration monitoring , wearable and flexible electronics

Introduction

Recent years have witnessed the explosive development of wearable sensors for monitoring human activities and healthcare services [1], [2]. Real-time health monitoring provides significant benefits for early-stage disease detection and cost-effective treatment [3]. The five traditional vital physiological indicators, generally considered essential to evaluate and monitor human health, are respiration rate, heart rate, body temperature, blood pressure and blood oxygen saturation [1]. Among these indicators, respiration rate provides a better evaluation to distinguish between stable and risky patients [1], [4]–[5][6]. Respiration rate is a critical sign in evaluating a person's health and detecting symptoms of respiratory diseases such as cardiac arrest, sleep apnea syndrome, chronic obstructive pulmonary disease and asthma [5], [7]. Detection of abnormal respiration rate can help to diagnose severe illness.

There are various approaches for respiration monitoring, which can be measured through either direct contact or noncontact methods [4], [7]. Noncontact methods have not been widely used in clinical setup because of concerns related to patient safety, complexity, and interference with other medical instruments [4]. On the other hand, contact methods can provide more reliable signals of respiratory sounds [8] or respiratory airflow [9], chest or abdominal movement [10]. Respiration airflow can be evaluated following differences in the temperature, humidity, or carbon dioxide concentration of exhaled and inhaled airs. Conventionally, airflow sensors were invasively inserted into patients' nostrils to measure the respiration rate, resulting in uncomfortable breathing. In recent years, the advances in wearable electronics for human-

activity monitoring and personal healthcare have increased their demands, not only on highly sensitive but also on comfort, flexibility and biocompatibility. Therefore, a bendable, high-performance and wearable sensor is the alternative for noninvasive real-time monitoring solution of respiration.

Carbon nanotubes (CNTs) have been considered as a promising material for wearable and flexible electronic devices owing to their lightweight, flexibility, superior mechanical strength [11] and outstanding electronic properties [12], [13]. Successful demonstrations on flexible and stretchable diodes [14], transistors [15], strain sensors [16], [17], thermoelectric portable devices [18], and displays [20] reported recently show enormous advancement in the development of CNT-based devices. Well-aligned and porous CNT films are ideal for temperature sensors thanks to its high temperature coefficient of resistance and high electrical conductivity [21]–[22][23]. However, the CNTs film is weak again mechanical contact, sensitive to deformation strain and bending; thus, it is challenging to use CNTs forest as a thin, wearable and flexible electronic devices.

This article proposes a bendable, sensitive and wearable flow sensor using highly oriented carbon nanotube films (HO-CNT) toward applications in human respiration monitoring. The sensing element of the HO-CNT flow sensor consisted of carbon nanotube films sandwiched between two polyacrylonitrile (PAN) nanofiber layers, which were then attached to a low-cost and flexible paper substrate. The nanofiber PAN, fabricated by electrospinning process, acted as very thin protective layers which had high mechanical strength but porous to promote the flow sensibility of the CNT. The sensor was investigated and applied as a respiration monitoring device, showing that it was bending proof, high flow-sensitivity, high signal to noise ratio (SNR) and rather fast response. Our sensor could also serve as a respiration monitoring device with reliability, stability and comfortability.

Sensor Design and Sensing Principle

Figure 1a presents the structure of the HO-CNT flow sensor. The sensor included the sensing element which was HO-CNT films protected by two PAN nanofiber layers. The sensing element was electrically connected to outside circuit via two electrodes made from conductive epoxy. The conductive epoxy easily deposited through the PAN layers making contact with the CNTs due to the porous structure of PAN nanofiber. All the sensing element and electrical contacts of the flow sensor were placed on a $95\,\mu m$ thick flexible paper substrate for accessibility, lightweight, biocompatibility, and disposable use.

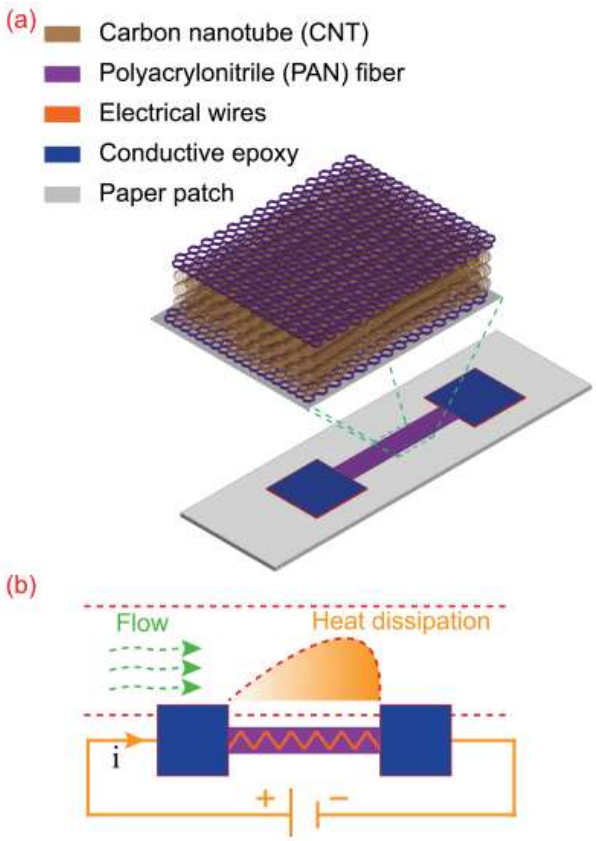

Fig. 1. The HO-CNT flow sensor operates based on the hotwire flow-sensing principle [9], [12], [22]–[23][24][25], Figure 1b. A current or a voltage was supplied to the HO-CNT film, which heated the HO-CNT film by the Joule effect. Its temperature rose and then reached a steady value when the heat loss to surrounding environment balanced the heat supply by Joule heating. As air flowed around the heated HO-CNT film, more heat was lost to the surrounding environment due to forced convection, resulting in a decrease in its temperature, hence changing resistance of the HO-CNT film. By evaluating resistance change of the heated HO-CNT film, the air flow velocity was measured.

Fabrication Process and Material Characterization

Figure 2a shows the fabrication process of the HO-CNT flow sensor. The fabrication process started with electrospinning the bottom PAN nanofiber layer (step-1). Charged threads of a PAN solution (consisting of copolymer polyacrylonitrile dissolved in dimethylformamide) were drawn out of the syringe by the electrostatic force induced by a voltage of 8 kV. The drawn threads were collected using a collector rotating at a speed of approximately 500 rpm, forming PAN nanofibers. In the next step, HO-CNT film was formed by pulling CNTs from a CNT wafer and placed them on the as-prepared PAN layer while spinning the collector. The top PAN layer then covered the HO-CNT film by the same electrospinning process. Next, we cut the $95\ \mu m$ thick paper patch and HO-CNT strip using a laser cutter, step-4. The final step assembled all components of the sensor. The HO-CNT strip was attached to the paper patch and electrical wires were connected to HO-CNT strip by silver epoxy electrodes. Whole experimental process was conducted by four-point measurement method as shown in Figure 2b.

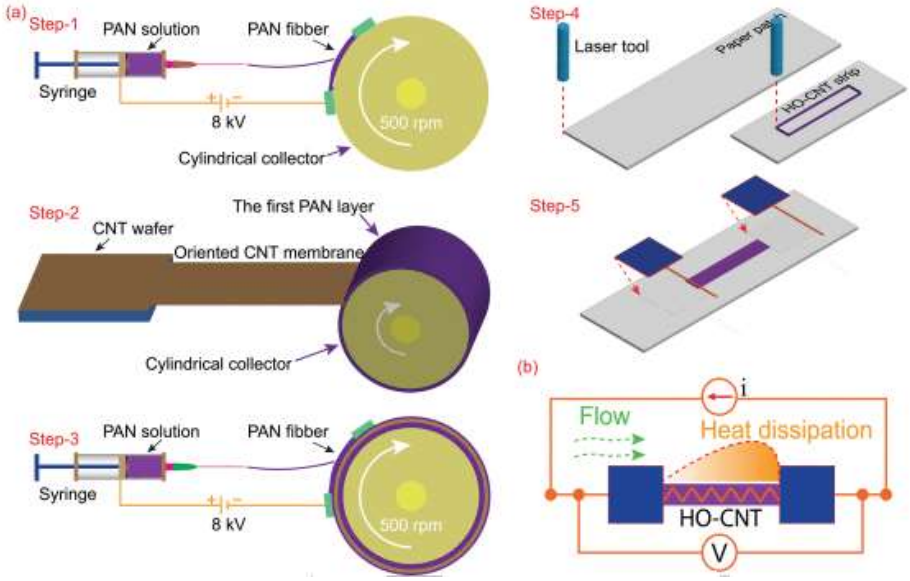

Fig. 2. **(a)** Fabrication process of the HO-CNT flow sensor. Step-1: Electrospinning the bottom PAN nanofiber layer. Step-2: Pulling and placing CNTs on the as-synthesized PAN layer. Step-3: Electrospinning the top PAN nanofiber layer. Step-4: Cutting CNT strip and paper patch. Step-5: Assembling the components. **(b)** Four-point measurement method.

The morphology of the HC-CNT flow sensor is shown in Figure 3. Figure 3a illustrates the scanning electron microscopy (SEM) image of the HO-CNT film pulled from the CNT forest wafer, clearly indicating that CNTs were well aligned along the same direction. As shown in Figure 3b, the PAN nanofiber layers completely covered the HO-CNTs, creating robust support and protection layers for HO-CNTs. Continuously collecting both HO-CNTs and PAN layers on the collector, Figure 3c, enabled mass-production. The Raman spectrum of the HO-CNTs, Figure 3d, reveals a D peak at the wavenumber of $1342 cm{-}1$ (carbon defects) and G peak at $1579 cm{-}1$ ($sp2$ hybridization of crystalline carbon) [26]. Porous structure of the PAN nanofiber layers is illustrated in Figure 3e. Because of the porous structure the conductive epoxy could easily diffuse through the PAN layers and created electrical interconnects between HO-CNTs. Moreover, the porosity of PAN nanofibers resulted in low density and fast heat transfer between HO-CNTs and the surrounding environment. Figure 3f shows optical images of the as-fabricated PAN-HO-CNT-PAN platform. The PAN-HO-CNT-PAN platform exhibits the good mechanical flexibility and robustness.

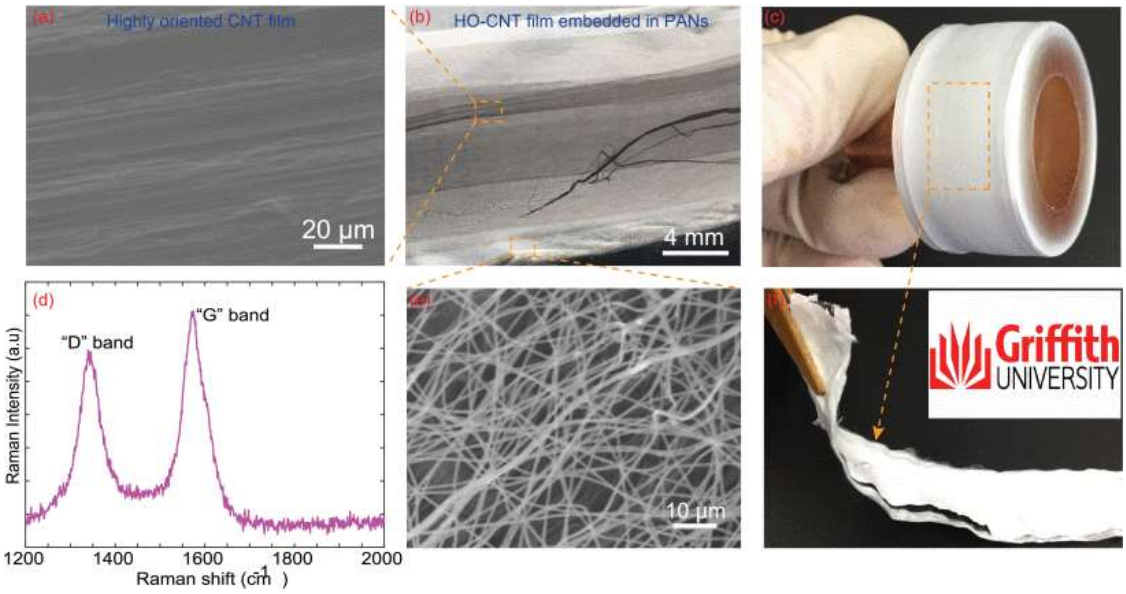

Fig. 3. Characterization of HO-CNTs embedded between two PAN nanofiber layers. (a) Scanning electron microscopy (SEM) image of the HO-CNT film. **(b)** HO-CNT film embedded in two PAN layers. **(c)** PAN-HO-CNT-PAN platform on the collector. **(d)** Raman spectrum of the CNTs. **(e)** SEM image of the PAN nanofibers. (f) The flexibility of as-fabricated PAN-HO-CNT-PAN structure

Results and Discussion

As the sensor was designed for respiration monitoring, its operating temperatures have to be lower than 80°C. The current-voltage (I-V) curves were characterized at various temperatures from room temperature to approximately 80°C as shown in Figure S1-a. The current linearly increased as the applied voltage varies from 0 to 1 V, which indicated good Ohmic contacts between the silver epoxy electrodes and the HO-CNT films. Change of the electric resistance of the HO-CNT film versus temperature was investigated as shown in Figure S1-b. The TCR (temperature coefficient of resistance) of the HO-CNT film was negative, an approximately 4 % decrease in resistance when the temperature rose from 22°C to 80°C.

A. Insensitive With Mechanical Disturbance

The flexibility is critical for sensors in human health monitoring applications, particularly human respiration monitoring. The accurate measurement of respiration rate will be difficult if the output signals are sensitive to deformation induced by bending. Hence, a wearable and flexible flow sensor that is insensitive with mechanical bending is desirable. The HO-CNT flow sensor was bent with various radius from 2 to 10 cm and the resistance and surface temperature were measured at the same time. Figure 4a shows the good stability of the resistance under mechanical loading. The resistance change was less than 0.4% across all bending experiments. As shown in Figure 4b, the temperature of the sensor also remained stable under different bending radii. The inset in Figure 4b shows the surface temperature distribution of the heated HO-CNT flow sensor with a maximum temperature of 60 °C. These results indicated that bending of the sensor due to wearing activities would not affect measurement results of respiration monitoring.

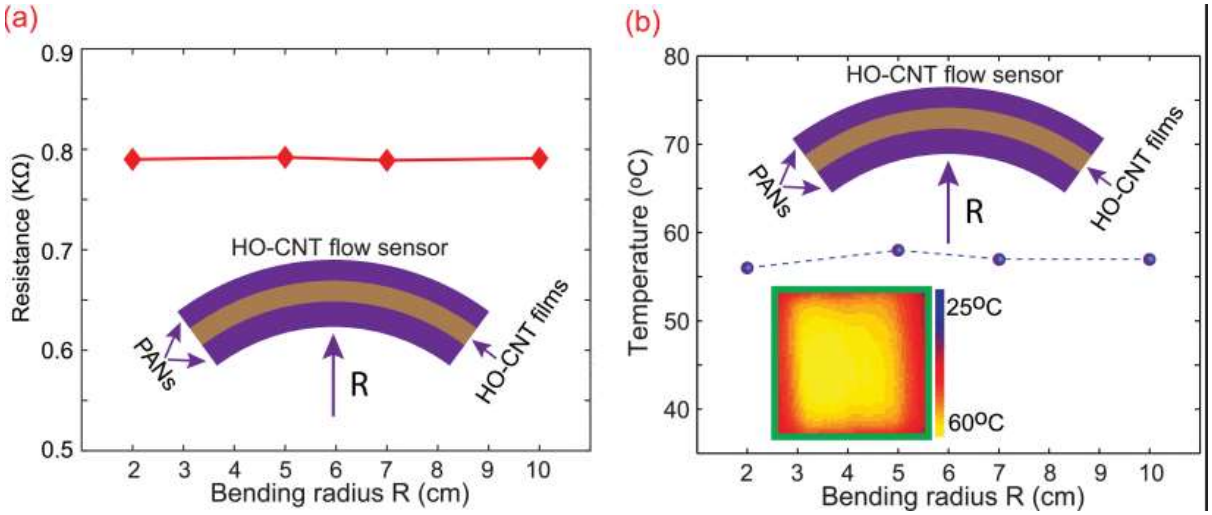

Fig. 4. Insensitivity of the HO-CNT flow sensor with mechanical bending. (a) Resistance stability to bending of the HO-CNT film. **(b)** Surface temperature stability to bending. The HO-CNT flow sensor was bent with bending radius from 2 to 10 cm and the resistance and the surface temperature of the sensor were monitored. The results show that the resistance and temperature were stable with difference bending radii

B. Performance of HO-CNT Flow Sensor

The HO-CNT flow sensor exhibited high sensitivity, fast response, high signal-to-noise ratio to airflow and excellent real-time response to human blowing. To evaluate performance of the airflow sensor, we monitored output voltage of the sensor responding to an airflow rate of 1.2 m/s under various supplied currents of 3 mA, 5 mA, and 7 mA. The flow sensitivity was estimated by the ratio of the absolute voltage change to applied airflow $s=\frac{|V-V_0|}{v}$, where V and V_0 are the output voltages at flow velocities of v and 0, respectively. As shown in Figure 5a, at the same flow velocities, a sharp response of the output voltage was generated as the airflow was applied with high signal-noise ratio. The voltage change was approximately 150 mV at a supplied current of 5 mA, and this value increased to 400 mV when supplied current rose to 7 mA. The airflow sensitivity was as high as 340 mV/(m/s) with the supplied current of 7 mA. This sensitivity was much higher than CNT thermal flow sensors reported previously [13], [26]. In addition, Figure 5b and Figure S2 show that the response time of the sensor (time lag taken to reach 90% magnitude of the signal) was less than 100 ms (bandwidth >10 Hz). The observed response time was relatively fast and suitable for the requirements of human respiration monitoring (breath rate of human being is from 12 to 20 times per minute). We further investigated the sensitivity of the sensor as a function of the supplied power. Figure 5c presents proportional relationship between resistance change and supplied power. The resistance change was approximately 0.05 % at an air velocity of 1.2 m/s for 1 mW power supply. The higher airflow sensitivity and bending-insensitivity can be qualitatively explained basing on the proposed equivalent circuit diagrams in Figure 5d-e. Figure 5d and Figure 5e show the schematic diagram of a layer of HO-CNT film and randomly aligned CNT film, respectively. The CNTs can be classified into two groups according to their alignment and contacts. Group 1 includes CNTs aligned perpendicular with the two electrodes and firmly connected with electrode (CNTs with yellow resistor symbol) and group 2 consists of CNTs do not directly contact with both two electrodes (CNTs with blue resistor symbol). CNTs in group 1 mainly and firmly contribute to the conductivity of the sensor while CNTs in group 2 depending their contacts with CNTs in group 1 might not contribute to the conductivity of the sensor. In addition, CNTs in group 1 firmly contact with the electrodes, hence their contributions to conducting carriers are stable under bending, while contacts between CNTs in

group 2 with CNTs in group 1 can be broken under bending. By aligning CNTs on one direction, most of CNTs in the HO-CNT flow sensor belong to group 1 (Figure 5d), resulting in more CNTs participating in conducting carriers and increasing the heat transfer area between sensor and surrounding environment. This made the HO-CNT flow sensor more sensitive with airflow and insensitive with bending. One the other hand, by randomly aligning CNTs, Figure 5e, there are less CNTs in group 1 resulting in smaller heat transfer areas or less sensitive with airflow and less stable with bending. Figure 5f depicts the real-time response of the HO-CNT flow sensor to human blowing. The output signal significantly changed under human blowing. The results indicate the capability of the sensor to recognize the input signals from human blowing.

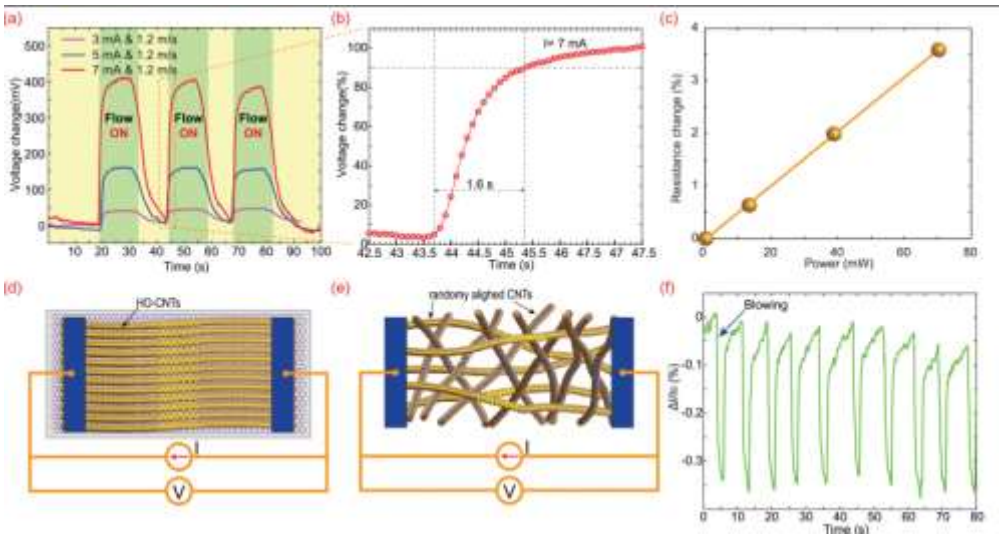

Fig. 5. Performance of the HO-CNT flow sensor. (a) Real time response of the measured output voltage to airflow of 1.2 m/s under different supplied currents. The sensitivity of the sensor was as high as 340 mV/(m/s) when supply current was 7 mA. **(b)** Response time of the sensor with the airflow, which was estimated as duration the voltage changing from 0 % to 90%. **(c)** Relationship between resistance change and power supply. The resistance change is approximately 0.05 % per 1 mW supplied power. **(d)** The proposed equivalent circuit diagram of the HO-CNT flow sensor. **(e)** The proposed equivalent circuit diagram of a randomly aligned CNT flow sensor. **(f)** The response of the flow sensor to human blowing.

C. Noninvasive Respiration Monitoring

The insensitive-bending property, high airflow sensitivity and good response to human blowing exhibited a great potential for respiration monitoring. To monitor respiration rate, the HO-CNT flow sensor was affixed to the philtrum of the testing subjects (Figure 6a). Because the sensor is thin, flexible, soft and lightweight, it was comfortable in wearing and did not disturb the breathing activity of the subjects while recording the real-time breathing patterns in different conditions with a high signal-to-noise ratio (SNR). All experiments regarding measurement of human respiration were performed in compliance with the relevant laws and institutional guidelines and approved by the Human Research Ethics Committee (HREC) of Griffith University.

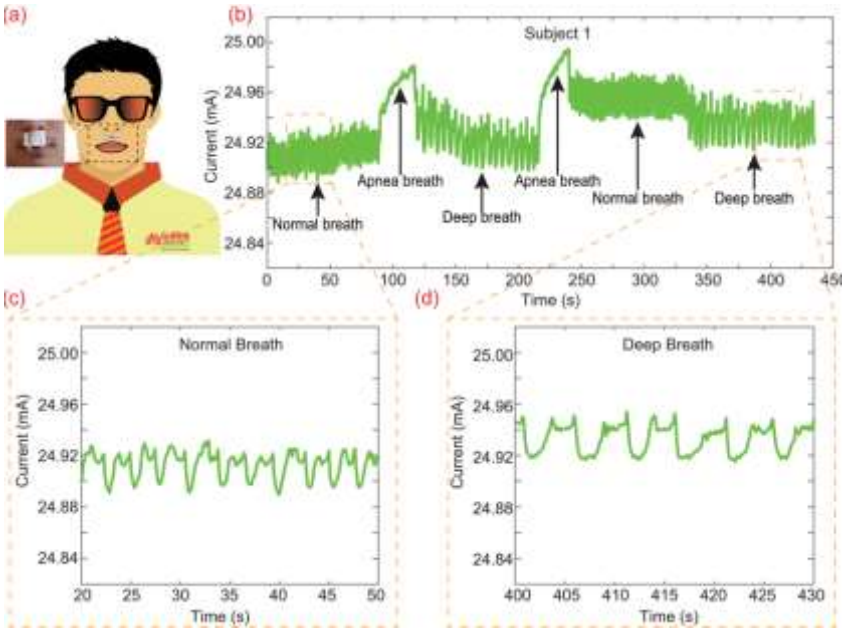

Fig. 6. Demonstration of respiration monitoring. (a) The HO-CNT flow sensor was attached to the philtrum of subject. **(b)** Response of the sensor to various breath patterns of the subject 1. Enlarged views of the sensor response to **(c)** normal breath and **(d)** deep breath pattern of the subject 1. The HO-CNT flow sensor can monitor real-time breath pattern of the subject 1. The different breath conditions were pointed out easily based on measured signals.

Figure 6b shows the breathing pattern of subject 1 who experienced different breathing conditions (normal breath, apnea breath and deep breath). Figures 6c and 6d are the enlarged views of the breathing patterns in periods of normal and deep breaths of subject 1, respectively. Respiration rate, estimated by the number of breaths per minute (bpm), is a critical parameter to appraise the breath quality. Figures 6c and 6d show that respiration rates of subject 1 were 21 bpm with normal breath and 12 bpm with deep breath. Another critical parameter to assess breath quality is the amplitude of breaths. As shown in Figures 6c and 6d, the airflow of subject 1's breath was almost similar in normal and deep breath. However, the duration of deep breath was longer than that of normal breath, so there was more air inhaled in deep breath condition. In addition, the HO-CNT flow sensors responded smoothly to the transition among durations of normal, deep, and apnea breaths. The breathing pattern of the subject 2 was also monitored and shown in Figure S3.

To evaluate the long-term stability of the HO-CNT flow sensor, we repeated the respiration monitoring experiment for many days with a duration of 30 minutes each day. Figures 7a, 7b, and 7c show response of the flow sensors to normal breath action of the subject 1 on the first day, one week later, and one month later, respectively. The results indicate that the HO-CNT flow sensor operates reliably for a long duration. The normal breathing patterns were almost identical for all experiments.

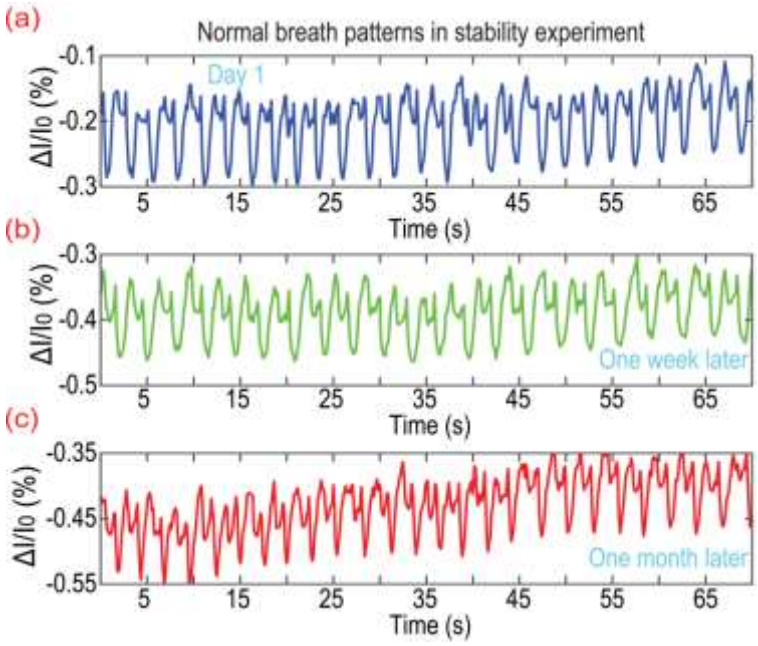

Fig. 7. Long-term stability of the flow sensor. Response of the sensor to normal breath of the subject 1 at **(a)** the first day 1, **(b)** one week later, and **(c)** one month later. The flow sensor operated stably over long time operation.

The reversibility and reproducibility of the HO-CNT flow sensor after bending were demonstrated as shown in Figure 8. Figure 8a depicts the response of the sensor to deep breath before bending and Figures 8b and 8c illustrate the performance of the sensor after 50 and 100 bending-cycles, respectively. No degradation in performance of the flow sensor was observed throughout the bending experiment.

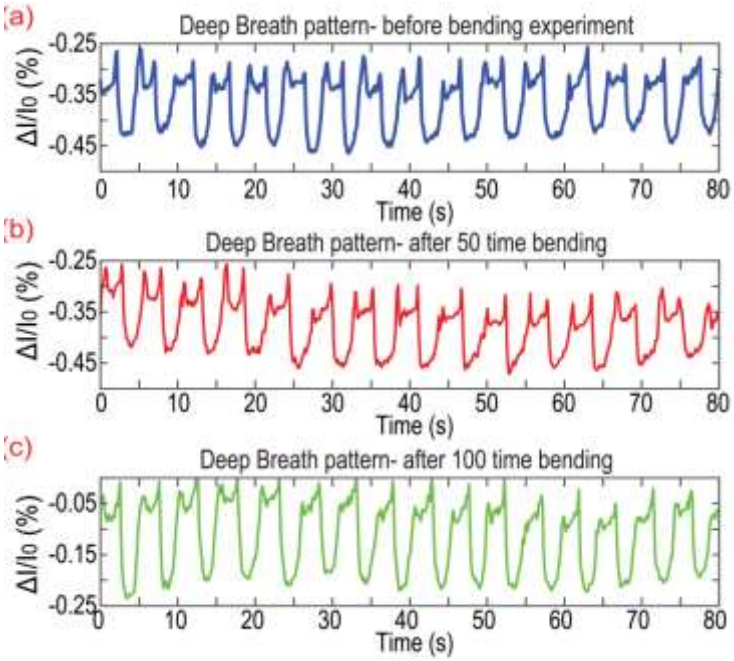

Fig. 8. Reversibility and reproducibility of the HO-CNT flow sensor to mechanical bending. The response of the sensor to deep breath of the subject 1 **(a)** before bending experiment, **(b)** after 50 time bending, **(c)** after 100 time bending. The performance of the HO-CNT flow sensor was perfectly remained throughout the bending experiment.

Conclusion

In summary, we have proposed a highly oriented carbon nanotube flow sensor, which is bending-insensitive, highly flow-sensitive, flexible, wearable, comfortable, bio-compatible and composable. The sensor exhibited a high sensitivity of 340 mV/(m/s) with airflow, insensitive to mechanical disturbance. We demonstrated that the sensor is suitable for respiration monitoring with high sensitivity, high signal-to-noise ratio, long-term stability and good durability.

References

1. T. Dinh et al., "Advances in rational design and materials of high-performance stretchable electromechanical sensors", *Small*, vol. 16, no. 14, Apr. 2020.

2. T. Dinh, T. Nguyen, H.-P. Phan, N.-T. Nguyen, D. V. Dao and J. Bell, "Stretchable respiration sensors: Advanced designs and multifunctional platforms for wearable physiological monitoring", *Biosensors Bioelectron.*, vol. 166, Oct. 2020.

3. H.-P. Phan et al., "Long-lived transferred crystalline silicon carbide nanomembranes for implantable flexible electronics", *ACS Nano*, vol. 13, no. 10, pp. 11572-11581, Oct. 2019.

4. D. Dias and J. P. S. Cunha, "Wearable health devices—Vital sign monitoring systems and technologies", *Sensors*, vol. 18, no. 8, pp. 2414, 2018.

5. F. Q. AL-Khalidi, R. Saatchi, D. Burke, H. Elphick and S. Tan, "Respiration rate monitoring methods: A review", *Pediatric Pulmonol.*, vol. 46, no. 6, pp. 523-529, Jun. 2011.

6. P. B. Lovett, J. M. Buchwald, K. Stürmann and P. Bijur, "The vexatious vital: Neither clinical measurements by nurses nor an electronic monitor provides accurate measurements of respiratory rate in triage", *Ann. Emergency Med.*, vol. 45, no. 1, pp. 68-76, Jan. 2005.

7. C. P. Subbe, R. G. Davies, E. Williams, P. Rutherford and L. Gemmell, "Effect of introducing the modified early warning score on clinical outcomes cardio-pulmonary arrests and intensive care utilisation in acute medical admissions", *Anaesthesia*, vol. 58, no. 8, pp. 797-802, Aug. 2003.

8. V. Balakrishnan et al., "Paper-based electronics using graphite and silver nanoparticles for respiration monitoring", *IEEE Sensors J.*, vol. 19, no. 24, pp. 11784-11790, Dec. 2019.

9. J. M. Shneerson, Sleep Medicine: A Guide to Sleep and Its Disorders, Hoboken, NJ, USA:Wiley, 2009.

10. T. Dinh et al., "Solvent-free fabrication of biodegradable hot-film flow sensor for noninvasive respiratory monitoring", *J. Phys. D Appl. Phys.*, vol. 50, no. 21, Jun. 2017.

11. G. K. Prisk, J. Hammer and C. J. L. Newth, "Techniques for measurement of thoracoabdominal asynchrony", *Pediatric Pulmonol.*, vol. 34, no. 6, pp. 462-472, Dec. 2002.

12. B. G. Demczyk et al., "Direct mechanical measurement of the tensile strength and elastic modulus of multiwalled carbon nanotubes", *Mater. Sci. Eng. A*, vol. 334, no. 1, pp. 173-178, Sep. 2002.

13. T. Dinh et al., "Environment-friendly carbon nanotube based flexible electronics for noninvasive and wearable healthcare", *J. Mater. Chem. C*, vol. 4, no. 42, pp. 10061-10068, 2016.

14. W. Obitayo and T. Liu, "A review: Carbon nanotube-based piezoresistive strain sensors", *J. Sensors*, vol. 2012, Apr. 2012.

15. D. Zhang et al., "Transparent conductive and flexible carbon nanotube films and their application in organic light-emitting diodes", *Nano Lett.*, vol. 6, no. 9, pp. 1880-1886, Sep. 2006.

16. E. Artukovic, M. Kaempgen, D. S. Hecht, S. Roth and G. Grüner, "Transparent and flexible carbon nanotube transistors", *Nano Lett.*, vol. 5, no. 4, pp. 757-760, Apr. 2005.

17. V. T. Dau, T. Yamada, D. V. Dao, B. T. Tung, K. Hata and S. Sugiyama, "Integrated CNTs thin film for MEMS mechanical sensors", *Microelectron. J.*, vol. 41, no. 12, pp. 860-864, Dec. 2010.

18. T.-K. Nguyen et al., "Electrically stable carbon nanotube yarn under tensile strain", *IEEE Electron Device Lett.*, vol. 38, no. 9, pp. 1331-1334, Sep. 2017.

19. V. T. Dau, D. V. Dao, T. Yamada, B. T. Tung, K. Hata and S. Sugiyama, "Integration of SWNT film into MEMS for a micro-thermoelectric device", *Smart Mater. Struct.*, vol. 19, no. 7, Jul. 2010.

20. S. Park, M. Vosguerichian and Z. Bao, "A review of fabrication and applications of carbon nanotube film-based flexible electronics", *Nanoscale*, vol. 5, no. 5, pp. 1727-1752, 2013.

21. A. Di Bartolomeo et al., "Multiwalled carbon nanotube films as small-sized temperature sensors", *J. Appl. Phys.*, vol. 105, no. 6, Mar. 2009.

22. T. Dinh, H.-P. Phan, A. Qamar, P. Woodfield, N.-T. Nguyen and D. V. Dao, "Thermoresistive effect for advanced thermal sensors: Fundamentals design considerations and applications", *J. Microelectromech. Syst.*, vol. 26, no. 5, pp. 966-986, Oct. 2017.

23. T. Dinh et al., "Polyacrylonitrile-carbon nanotube-polyacrylonitrile: A versatile robust platform for flexible multifunctional electronic devices in medical applications", *Macromol. Mater. Eng.*, vol. 304, no. 6, Jun. 2019.

24. V. Balakrishnan et al., "A hot-film air flow sensor for elevated temperatures", *Rev. Sci. Instrum.*, vol. 90, no. 1, Jan. 2019.

25. V. Balakrishnan, T. Dinh, H.-P. Phan, D. V. Dao and N.-T. Nguyen, "Highly sensitive 3C-SiC on glass based thermal flow sensor realized using MEMS technology", *Sens. Actuators A Phys.*, vol. 279, pp. 293-305, Aug. 2018.

26. H. Wang et al., "Bioinspired fluffy fabric with in situ grown carbon nanotubes for ultrasensitive wearable airflow sensor ", *Adv. Mater.*, vol. 32, no. 11, Mar. 2020.